

Figure S1. Expression levels of miR-27a-3p and miR-23a/27a/24-2 cluster members in clinical cervical cancer and normal tissues. (A) Relative expression of the members from the miR-23a/27a/24-2 cluster based on TCGA-CESC dataset (309 cervical cancer tissues and 3 normal cervical tissues). The P-value was calculated using Wilcoxon rank sum tests. (B) Relative expression of miR-27a-3p, miR-23a-3p and miR-24 based on the GSE20592 dataset, which included 29 paired cervical cancer tissues and its adjacent normal tissues. (C) Relative expression of miR-27a-5p, miR-23a-3p/5p and miR-24-2-5p based on GSE86100, which included 6 cervical cancer tissues and 6 normal tissues. (B and C) Data were analyzed using a two-tailed Student's t-test; $P < 0.05$ was considered to indicate a significant difference; * $P < 0.05$, ** $P < 0.01$, ns, not significant. TCGA-CESC, The Cancer Genome Atlas (TCGA)-Cervical Squamous Cell Carcinoma and Endocervical Adenocarcinoma (CESC).

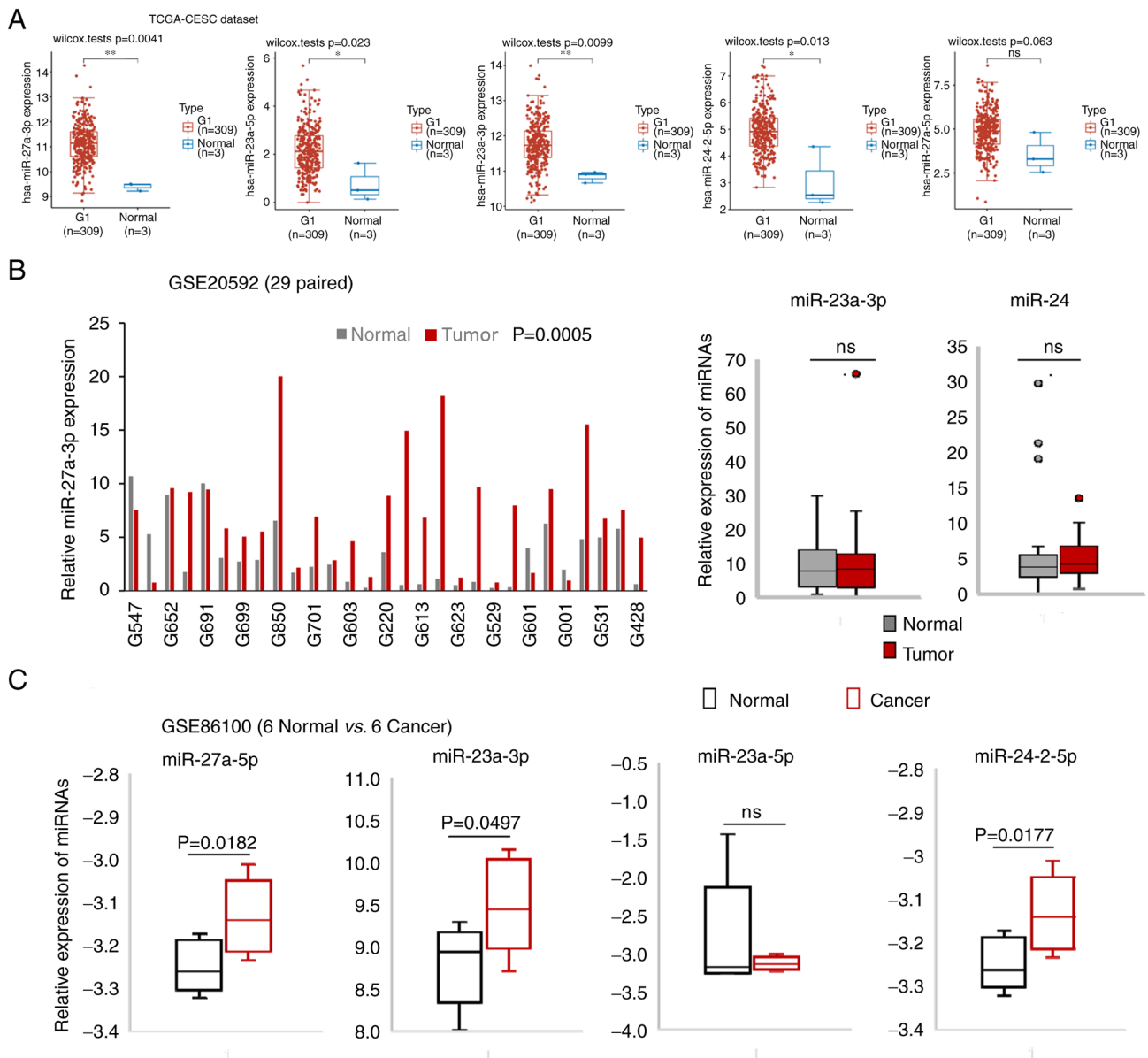


Figure S2. miR-27a-3p binds to the 3'UTRs of MAP3K14 and TRAF3, and upregulates their expression in cervical cancer cells. (A) The sequence alignment of miR-27a-3p with the wild-type (wt) and the mutated (mut) target sequences of MAP3K14, as well as TRAF3. The seed sequences of miR-27a-3p are highlighted in red, and the mutated bases are underlined and are shown in bold font. (B) The relative EGFP fluorescent intensities of 3'UTR reporters (MAP3K14 and TRAF3) were significantly upregulated by miR-27a-3p, and the increased EGFP intensities were abolished by the mutated constructs, respectively, indicating the direct binding of miR-27a-3p to their 3'UTRs. (C) Reverse transcription-quantitative assays indicated the significantly increased or decreased mRNA expression levels of MAP3K14 and TRAF3 upon miR-27a-3p modulation. (D) Representative western blot demonstrated the increased expression of MAP3K14 and TRAF3 upon the ectopic expression of miR-27a-3p in HeLa cells. The numbers under the western blot bands indicate the relative quantifications normalized to the loading control. * $P < 0.05$, ** $P < 0.01$ and *** $P < 0.001$, vs. their respective controls. TRAF3, TNF receptor associated factor 3; MAP3K14, mitogen-activated protein kinase kinase kinase 14.

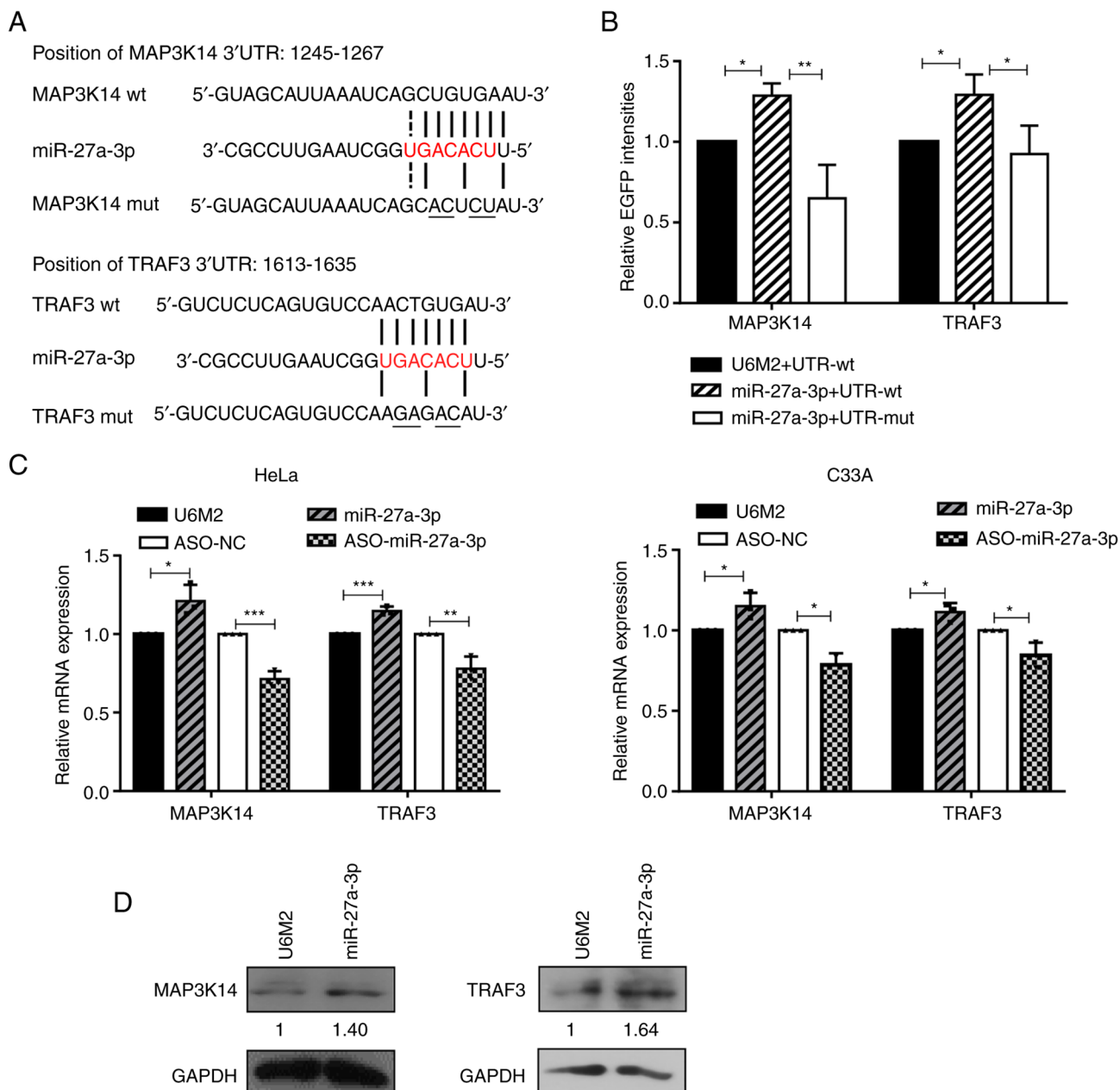


Figure S3. Survival analyses based on TCGA-CESC dataset. (A) Overall and disease-free survival curves obtained from GEPIA2 based on MAP3K14, TAB3 and TRAF3 expression levels. (B) Overall and disease-free survival analyses based on miR-27a-3p expression using the HiPlot online drawing tool. TCGA-CESC, The Cancer Genome Atlas (TCGA)-Cervical Squamous Cell Carcinoma and Endocervical Adenocarcinoma (CESC); TAB3, TGF- β activated kinase 1 binding protein 3; TRAF3, TNF receptor associated factor 3; MAP3K14, mitogen-activated protein kinase kinase kinase 14.

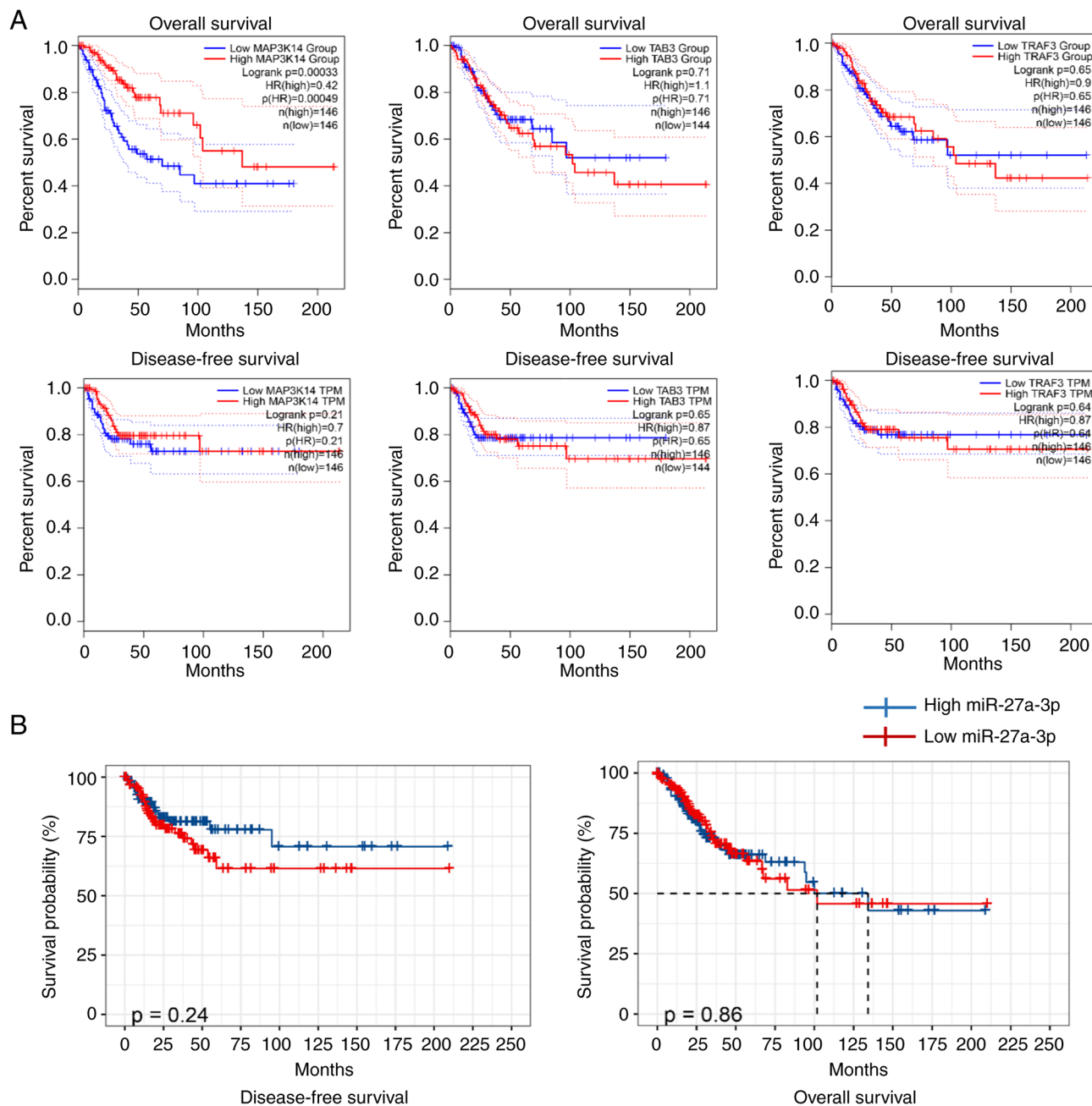


Figure S4. The upregulated expression of TAB3 induced by miR-27a-3p is partially dependent on AGO2, and AGO2 inhibition decreases the global expression of TAB3. (A) Western blot analysis was performed to verify the efficiencies of the constructed shRNA vectors for silencing AGO2, and shR1-AGO2 was selected for further analyses. (B) The upregulation of TAB3 induced by miR-27a-3p occurred in an AGO2-dependent manner, and the silencing of AGO2 resulted in the reduction of TAB3 expression. The numbers under the western blot bands indicate the relative quantifications normalized to their loading control. AGO2, Agonaute 2; TAB3, TGF- β activated kinase 1 binding protein 3.

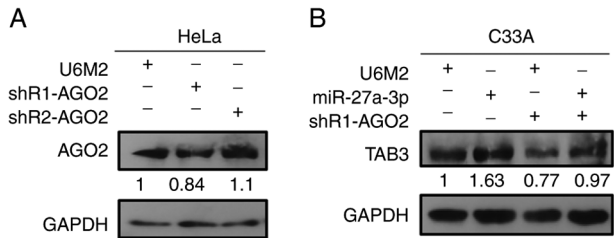


Figure S5. Verification of the promoter activity of miR-27a and its regulation by the NF- κ B transcription factor subunit, NFKB1. (A) The constructed pGL3-P2 had a significantly higher relative luciferase activity compared with pGL3-P1. (B) The efficiencies of KBE-p50, shR-NFKB1, KBE-p65 and shR-p65 were evaluated using western blot analysis. The numbers under the western blot bands indicate the relative quantifications normalized to their loading control. (C) The silencing of NFKB1 significantly decreased the promoter activity of the fragment P2. (D) NFKB1 suppression resulted in the decreased promoter activity of fragment P2-F509, but not the p65 binding site-depleted construct (F509-Del1546), and the increased effects induced by the overexpression of NFKB1/p50 were also decreased to a certain degree due to the p65 binding site depletion. * $P < 0.05$, ** $P < 0.01$ and *** $P < 0.001$, vs. their respective controls. ns, not significant.

